# Are superluminous Supernovae and long GRBs the Products of dynamical Processes in young dense Star Clusters?

van den Heuvel, E.; Portegies Zwart, S.F.

DOI
10.1088/0004-637X/779/2/114

Publication date
2013

Document Version
Final published version

Published in
Astrophysical Journal

The Astrophysical Journal, 779:114 (9pp), 2013 December 20 doi:10.1088/0004-637X/779/2/114


# ARE SUPERLUMINOUS SUPERNOVAE AND LONG GRBs THE PRODUCTS OF DYNAMICAL PROCESSES IN YOUNG DENSE STAR CLUSTERS?

E. P. J. van den Heuvel[1,2] and S. F. Portegies Zwart[3]
[1] Astronomical Institute Anton Pannekoek, University of Amsterdam, P.O. Box 94249, 1090 GE Amsterdam, The Netherlands
[2] Kavli Institute for Theoretical Physics, UCSB, Santa Barbara, CA 93106-4030, USA
[3] Leiden Observatory, Leiden University, P.O. Box 9513, 2300 RA Leiden, The Netherlands
*Received 2013 March 21; accepted 2013 October 27; published 2013 December 2*

## ABSTRACT

Superluminous supernovae (SLSNe) occur almost exclusively in small galaxies (Small/Large Magellanic Cloud (SMC/LMC)-like or smaller), and the few SLSNe observed in larger star-forming galaxies always occur close to the nuclei of their hosts. Another type of peculiar and highly energetic supernovae are the broad-line Type Ic SNe (SN Ic-BL) that are associated with long-duration gamma-ray bursts (LGRBs). Also these have a strong preference for occurring in small (SMC/LMC-like or smaller) star-forming galaxies, and in these galaxies LGRBs always occur in the brightest spots. Studies of nearby star-forming galaxies that are similar to the hosts of LGRBs show that these brightest spots are giant H II regions produced by massive dense young star clusters with many hundreds of O- and Wolf-Rayet-type stars. Such dense young clusters are also found in abundance within a few hundred parsecs from the nucleus of larger galaxies like our own. We argue that the SLSNe and the SNe Ic-BL/LGRBs are exclusive products of two types of dynamical interactions in dense young star clusters. In our model the high angular momentum of the collapsing stellar cores required for the engines of an SN Ic-BL results from the post-main-sequence mergers of dynamically produced cluster binaries with almost equal-mass components. The merger produces a critically rotating single helium star with sufficient angular momentum to produce an LGRB; the observed "metal aversion" of LGRBs is a natural consequence of the model. We argue that, on the other hand, SLSNe could be the products of runaway multiple collisions in dense clusters, and we present (and quantize) plausible scenarios of how the different types of SLSNe can be produced.

*Key words:* galaxies: starburst – galaxies: star clusters: general – gamma-ray burst: general – globular clusters: general – supernovae: general

*Online-only material:* color figures

## 1. INTRODUCTION

In the past decades several new and rare types of extremely bright and peculiar supernovae (SNe) have been discovered.

1. The broad-line Type Ic SNe (abbreviated as SNe Ic-BL) that are associated with long-duration gamma-ray bursts (abbreviated as LGRBs). This was the first extremely bright type of SN discovered (Galama et al. 1998; Wolf & Podsiadlowski 2007; Gehrels & Mészáros 2012; Kouveliotou et al. 2012). They have no H and often also no He in their spectra and are characterized by extremely large outflow velocities ($\sim$40,000 km s$^{-1}$), implying very large kinetic energies ($\sim 10^{52}$ erg). When they are associated with an LGRB (also a number have been discovered that are not; see below), they are related to the explosions of rapidly rotating, almost pure CO stars with masses $>5\ M_{\odot}$, almost bare cores of originally very massive stars (Iwamoto et al. 1998), and the prototype SN 1998bw/GRB 980425 ejected of order half a solar mass of $^{56}$Ni (Cano et al. 2011). Since the discovery of the LGRB-related SNe of Type Ic-BL, also non-GRB SNe of this type have been discovered, in general in low-redshift galaxies ($\langle z \rangle \sim 0.04$; Graham & Fruchter 2013). They are thought to have the same central engines that in LGRBs produce relativistic jets (Soderberg et al. 2010); the jets are thought to be unable to penetrate the outer layers of the star and to deposit their energy mostly inside the star, producing an SN Ic-BL (Soderberg et al. 2010; Levesque et al. 2010b).
2. The so-called superluminous SNe (SLSNe), a new class of SNe discovered with the recent large-scale surveys for transients. The several tens of extremely energetic and bright SLSNe that are now known have bolometric luminosities up to some 50 times those of Type Ia SNe (Gal-Yam 2012). There are at least three classes of SLSNe: the SLSN-I, which lack hydrogen in their spectra; the SLSN-II, which do have H in their spectra; and the SLSN-R, which have a long light-curve tail powered by the radioactive decay of a very large amount of $^{56}$Ni, typically of order 5 $M_{\odot}$ (for a review, see Gal-Yam 2012).

Both the SLSNe and the LGRBs (as well as their SN Ic-BL counterparts) have in common that (1) they are very rare: the rate of LGRBs ($10^{-7}$ Mpc$^{-3}$yr$^{-1}$) is some $10^3$ times lower than the core-collapse SN rate (the non-GRB SN Ic-BL may be one to two orders of magnitude more common, e.g., see Graham & Fruchter 2013, but still rare). The combined rate of the SLSNe is of order $10^{-8}$ Mpc$^{-3}$ yr$^{-1}$, some $10^4$ times lower than the core-collapse SN rate. These rates imply that a rare type of stellar evolution is required to produce these events. (2) Both the LGRBs and SLSNe occur almost exclusively in small star-forming galaxies (Small/Large Magellanic Cloud (SMC/LMC)-like or smaller; the same appears to be true for the non-GRB SN Ic-BL; Kelly & Kirshner 2012). Fruchter et al. (2006) found that in 41 out of 42 studied LGRBs the host is a small star-forming galaxy. Only one LGRB host is a grand-design spiral galaxy, and it was found that in their small hosts the GRBs fall on optically bright spots. Studies of nearby small starburst galaxies show that such bright spots are clumps of massive O

and Wolf-Rayet (W-R) stars. For example, NGC 3125 has a number of such clumps with spectra that are a mixture of O and W-R spectra (Hadfield & Crowther 2006). Studies of these clumps show that such small galaxies may harbor as many as $10^4$ O and W-R stars, which are concentrated in a small number (three to six) of massive young star clusters, with masses of order $10^5\ M_\odot$ each, and each containing often >600 O stars.

The SLSNe share the property of the LGRBs to occur almost exclusively in small starburst galaxies. The only two SLSN-II that reside in larger Milky-Way-type galaxies were found very close to the nucleus of their hosts (Drake et al. 2011; Gal-Yam 2012). Gal-Yam (2012) remarks that this "*suggests that to produce SLSNe perhaps special conditions are required that are unique to this environment (e.g., circumnuclear star-forming rings), somehow mimicking the conditions in star-forming dwarf galaxies.*" Indeed, in the inner few hundred parsecs of the bulges of many larger galaxies, nuclear starbursts are going on. Seyfert galaxies and our own Galaxy are prime examples (Conti et al. 2008). Within 100 pc from the center of our Galaxy many massive young star clusters are present, of which the Arches and Quintuplet clusters are key examples. These clusters in our Galaxy's central region are massive, but even more important (as we will argue in Section 3.1) is their very high stellar density, which in the core of Arches exceeds $10^6\ M_\odot \mathrm{pc}^{-3}$. Such a high star density is also characteristic of the young clusters in small star-forming galaxies like the LMC and in the central regions of starburst galaxies like M82 (Lim et al. 2013).

The LMC cluster R136, in the 30 Doradus region, has a high density. The reason why the clusters in small star-forming galaxies reach such high star densities may be related to the power in the turbulent velocity spectrum, which leads to a shorter free-fall timescale of the gas than in the disks of large galaxies (Kaaret et al. 2011). In the high-density star-forming regions, the turbulent energy spectrum is a power law $E(k) \propto k^{-\gamma}$ in which $\gamma = 1.85 \pm 0.04$ (Padoan et al. 2009) rather than the usual $\gamma \gtrsim 3$ (McKee & Ostriker 2007) (with more power in the large-scale gas motion). This is consistent with the results of hydrodynamical simulations of the formation of star clusters in which a turbulent velocity field with more power at small structures stimulates the formation of dense clusters (Brunt et al. 2009; Bate 2009; Moeckel & Bate 2010; Federrath & Klessen 2012).

This effect can be observed in the population of star clusters in nearby galaxies, by fitting their number $N$ to the Schechter function, which takes the form (Schechter 1976)

$$N dM \propto M^\beta \exp(M/M_*). \quad (1)$$

The distribution of the masses of young ($\lesssim$10 Myr old) star clusters in large quiescent galaxies, like M31, is best represented by a Schechter function with a characteristic mass $M_* \simeq 2\times10^5\ M_\odot$ and with an exponential falloff of $\beta \lesssim -3$, whereas for dwarf starburst galaxies and interacting galaxies like M51 $\beta \sim -2$ (Portegies Zwart et al. 2010). In Figure 1 (see also Section 4) we present the probability density function of cluster birth mass and size. The gray shades represent the convolution of the Schechter mass function (Equation (1)) with a lognormal distribution for the cluster sizes. For the former, we adopted $\beta \lesssim -3$ and $M_* \simeq 2\times10^5\ M_\odot$. For the lognormal size distribution, we adopted a mean cluster radius of 5 pc with a dispersion of 3 pc, which is consistent with the observed young ($\lesssim$10 Myr) star clusters in the Local Group (Portegies Zwart et al. 2010). We speculate that the dense torus of inspiraling gas accumulating in the central few hundred pc of the bulges of spiral galaxies may also have a turbulent velocity structure, due to the high local star formation and associated high SN rate.

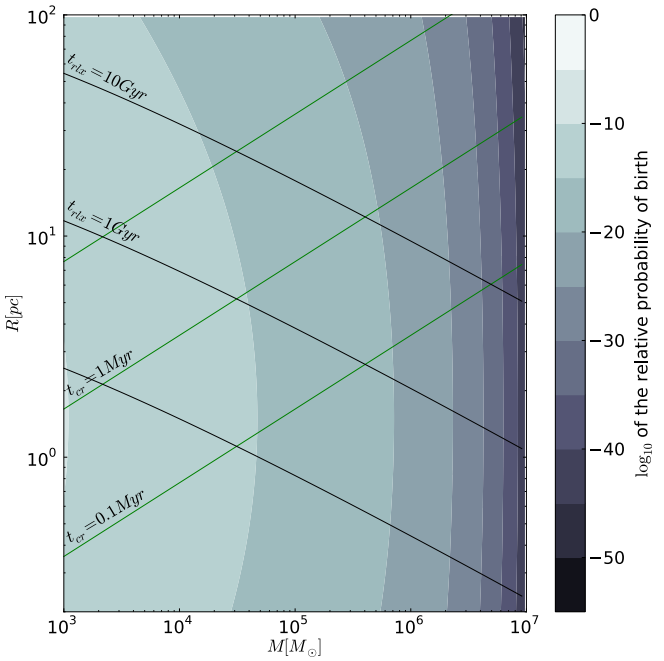


**Figure 1.** Birth conditions (in mass and size) of Milky Way star clusters. Gray shades (scale to the right) give the logarithm of the relative probability of birth. The birth probability density function is a convolution of the cluster initial mass function (Schechter function (Equation (1)) with $M_* = 2\times10^5\ M_\odot$ and $\beta = -3$) and the size distribution (lognormal with a mean of 5 pc and a dispersion of 3 pc). The black curves (top left to bottom right) give the cluster two-body relaxation time, with $t_{\rm rlx} = 10$ Gyr for the top curve down to 100 Myr for the bottom curve. The green curves (bottom left to top right) give the cluster crossing time, with $t_{\rm cr} = 10$ Myr for the top curve down to 0.1 Myr for the bottom curve.

(A color version of this figure is available in the online journal.)

It therefore appears that both the LGRBs/SN Ic-BL and the SLSNe solely occur in regions of galaxies where very dense young star clusters are present. This suggests that both types of objects could be the products of evolutionary processes that are unique to dense massive young star clusters and do not occur anywhere else (this suggestion for the LGRBs was casually made to one of us by S. Kulkarni in 2006). We present later in this paper (see Section 3) a possible scenario of how this could come about and quantize the effect in Sections 3.1 and 5. But before that, in Section 2, we consider the boundary conditions set by the observations, for models for producing LGRBs/SN Ic-BL.

## 2. CONDITIONS REQUIRED FOR PRODUCING LGRBs/SN Ic-BL

The general consensus on the conditions required for producing a long GRB is the collapse of a very rapidly rotating, almost bare CO core of a massive star. There is strong observational evidence that the GRB is produced by a narrowly collimated relativistic jet with a Lorentz factor of order $10^2$–$10^3$ (Woosley & Bloom 2006; Gehrels & Mészáros 2012). The beam opening half-angle of 5°–10° leads to a beaming fraction of order 0.003. There are two models for producing such jets.

1. According to the "*collapsar*" model of Woosley (1993), in which a very massive rapidly rotating core collapses to a black hole, the core has so much angular momentum that

not all of the core matter can at once disappear into the black hole. Part of the core matter then temporarily forms a disk of nuclear matter around the black hole. Viscous and/or magnetic dissipation in this disk drive, in combination with frame dragging, a relativistic jet, which results in the GRB (MacFadyen & Woosley 1999).

2. A model in which the very rapidly rotating core collapses to a strongly magnetized neutron star (magnetar) that is spinning with a period of order of a millisecond (Metzger et al. 2011; Zhang & Yan 2011). The spin-down energy loss by magnetic dipole emission and the relativistic wind of such an extreme pulsar is so gigantic that it will spin down to a long period on a timescale of minutes to hours and produce energetic electromagnetically powered relativistic jets along the rotation axis, and it also blows up the star in an SN Ic-BL (Metzger et al. 2011; Gehrels & Mészáros 2012; see also Kasen & Bildsten 2010; Woosley 2010).

Both these models require that in order to produce an LGRB, the collapsing massive CO core must have high angular momentum, in the range $10^{16}$–$10^{18}$ cm$^2$ s$^{-1}$ (Woosley & Bloom 2006; Kouveliotou et al. 2012). Since all SN Ic-BL are thought to have the same central engine that produces highly relativistic jets (see above), also the non-GRB SNe of this type must have collapsing CO cores with the same high angular momentum. Two possible ways have been suggested for the core of a massive star to obtain such high angular momentum: either (1) very low metallicity (e.g., Yoon & Langer 2005) or (2) evolution in a close binary system (e.g., Fryer et al. 2007; van den Heuvel & Yoon 2007; Bogomazov et al. 2007; Detmers et al. 2008). In the first type of models, it is argued that low metallicity gives weak stellar winds such that the winds do not carry off much angular momentum and the star keeps high angular momentum throughout its life. Its rapid rotation in these models keeps the star completely mixed, such that it evolves homogeneously and may in the end become a rapidly rotating CO star that collapses (Yoon & Langer 2005; Langer & Norman 2006; Yoon et al. 2006).

The requirement of very low metallicity is fulfilled for many of the host galaxies of LGRBs, but there are also several with almost solar metallicity (Wolf & Podsiadlowski 2007; Gehrels & Mészáros 2012) and the requirement of low metallicity must be reconsidered (Hao & Yuan 2013). Simultaneously, the hosts of the non-GRB SNe of type Ic-BL tend to have low metallicity as well (e.g., Graham & Fruchter 2013; Kelly & Kirshner 2012); however, some have metallicities as high as 1.7–3.5 times solar, while still having the same central engine (Levesque et al. 2010b). Therefore, it seems likely that low metallicity, although it appears to facilitate the production of an LGRB and SN Ic-BL, is not the only factor involved in the production of these phenomena, which require a high angular momentum of the collapsing stellar core (see below).

### 2.1. Gamma-Ray Bursts and SN Ic-BL from Regular versus Dynamically Formed Binaries

In close binary models—involving late evolutionary phases of normal massive binaries—tidal forces keep the star in synchronous (rapid) rotation (e.g., van den Heuvel & Yoon 2007), or a rapidly rotating merger product is produced ("Helium merger GRB"; Fryer et al. 2007). The main argument against these models, which involve the *regular* evolution of binaries that started out as normal massive systems, is that such binaries are found throughout the disks of all spiral galaxies. Therefore, if these models would work, one would expect many LGRBs to be seen in disks of spiral galaxies (since a large part of the present-day star formation is thought to take place in these galaxies; e.g., see Conti et al. 2008), contrary to what is observed. Therefore, models based on *normal* massive binary evolution cannot comply with the boundary conditions set by the environments where LGRBs/SN Ic-BL are found.

The main open questions that then remain are (1) why do LGRBs (and other engine-driven SN Ic-BL) occur in small star-forming galaxies, and (2) why do LGRBs have a preference for low metallicities, while not all SN Ic-BL share this preference?

We propose that the answers to these questions are that the rapidly rotating CO cores required for the engines of SN Ic-BL are solely produced in mergers of a special type of binaries that result from gravitational dynamical processes that occur only in dense, young massive star clusters. It turns out that dynamical processes tend to produce close binaries with almost equal-mass components ($q \simeq 1$).

In order for both stars to have a helium-burning helium core at the time of the merger, the less massive star of the two should already have left the main sequence (have exhausted hydrogen in its core), while the more massive one should not yet have terminated core helium burning. By performing a series of stellar evolution calculations using MESA (Paxton et al. 2011) from AMUSE framework (Portegies Zwart et al. 2013) with solar ($Z_\odot$) and subsolar (0.3 $Z_\odot$) metallicity, we find that the two stars should not differ more than 20% in mass, although the result is somewhat mass dependent, allowing a larger mass difference for more massive stars: the mean of the minimum mass ratio is $q \gtrsim 0.87 \pm 0.07$ for solar metallicity and $q \gtrsim 0.89 \pm 0.06$ for subsolar. This poses a lower limit for the required mass ratio. The merger of such a binary produces a rapidly rotating massive helium star, and we show that these stars at the time of core collapse can still have the required high core angular momentum, and that their event rates match the observed rates of SN Ic-BL. The winds of helium stars (W-R stars) carry off part of their original angular momentum. We show that because of the metallicity dependence of the wind mass-loss rates of W-R stars, at low metallicity high final core angular momentum occurs over a much larger range of helium star masses than at high metallicity. Therefore, this model favors the occurrence of LGRBs at low metallicity, but does not exclude high metallicities. An additional factor favoring low metallicity is that the helium merger product is more easily produced at low than at high metallicity (see Section 2.2).

### 2.2. The Evolution of the Specific Angular Momentum of a Post-merger Helium Star, Resulting from an Almost Equal-mass Binary

We used the models for the evolution of helium stars in the mass range 8–32 $M_\odot$ of Arnett (1978) and for larger mass values the models of Deinzer & Salpeter (1964; models computed with more recent evolution codes produce very similar results). The total lifetimes, helium-burning core masses, radii, and luminosities of these models were adopted, and for other helium star mass values in the range 8–100 $M_\odot$, these quantities were calculated by logarithmic interpolation and extrapolation from these values as a function of the logarithm of mass. We assumed that at the time of the merger of the helium stars (cores of their progenitors) the merger product helium star is on the zero-age helium main sequence and is rotating with a breakup angular velocity $\Omega$. This is a natural consequence, because at

the time of the merger the two helium cores are orbiting each other with Keplerian velocities; the merger therefore results in a single helium star rotating with a Keplerian equatorial angular velocity, which is the maximum possible "breakup" rate. The assumption that they start on the zero-age helium main sequence implies that after their formation these stars have the longest possible lifetimes and therefore undergo the maximum possible amount of stellar-wind mass loss (and thus maximum angular momentum loss) that such a merger product can experience. (The real angular momentum loss of these merger products will therefore always be smaller than we calculate here, and their final core angular momentum will always be larger than we calculate here). For the wind mass-loss rates, we adopted the metal-dependent mass-loss rates of WN-type W-R stars as given by Yoon et al. (2006):

$$\log(\dot{M}_{\rm W\text{-}R}/[M_\odot\,{\rm yr}^{-1}]) = -12.95 + 1.5\log(L/L_\odot) + 0.86\log(Z/Z_\odot). \quad (2)$$

Here $Z$ and $Z_\odot$ indicate the star's metallicity and the Sun's metallicity, respectively.

This mass-loss rate was adopted until the mass of the helium star had been reduced to the mass of the convective burning core that it had at the start of its evolution. Since in this core carbon is produced, we assumed that from here on the W-R star becomes a carbon type WC star. For these stars we adopted the wind mass-loss rates for WC stars given by Conti et al. (2008).

For $Z = Z_\odot$, these rates are equal to the WN mass-loss rates given by Equation (2); for $Z = 0.3\,Z_\odot$ they are three times the rate given by Equation (2) for this metallicity, and for $Z = 0.1\,Z_\odot$ they are six times the rate given by Equation (2) for this metallicity.

We assumed the wind particles to carry off the angular momentum that they had at the surface of the star, and since the bulk of the masses of helium stars are convective, we assumed the stars to be rotating as a solid body until the moment of helium exhaustion in the convective core. After this, the contracting carbon–oxygen core will spin up, but its rotation will be braked by coupling to the layers around it. As a result, it will lose part of the angular momentum it had at the time of the helium exhaustion. After the end of carbon burning, at the time of core collapse, it will still have a fraction $f$ of the specific angular momentum that it had at helium exhaustion. We adopted the values of $f$ as given by S.-C. Yoon (2006, private communication), who calculated the evolution of rotating helium stars with masses between 8 and 40 $M_\odot$ using Spruit's (2002) mechanism for core-envelope coupling. He found that the inner 3 $M_\odot$ of the CO cores of these stars at the moment of the core collapse have retained a fraction $f$ of their initial specific angular momentum that these had as a helium star in solid-body rotation. These $f$-values are as follows: for $m_{\rm He} = 8$–$16\ M_\odot$, $f = 0.20$; for $m_{\rm He} = 20\,M_\odot$, $f = 0.40$; for $m_{\rm He} = 25\ M_\odot$, $f = 0.65$; and for $M_{\rm He} = 40\ M_\odot$, $f = 0.75$. For all masses $>40\ M_\odot$ we adopted $f = 0.75$, and for other masses we estimated the $f$-values by logarithmic interpolation as a function of logarithm of the mass.

The angular momentum of a star of mass $m$ and radius $r$, rotating at angular velocity $\Omega$, is

$$J = mk^2r^2\Omega. \quad (3)$$

Here $k$ is the radius of gyration of the star, which for helium stars is given by Savonije & van den Heuvel (1977), as follows: for 8 $M_\odot$, $k^2 = 0.100$; for 16 $M_\odot$, $k^2 = 0.115$; and for $M = 32\ M_\odot$ and larger, $k^2 = 0.130$. For masses between 8 and 32 $M_\odot$ the $k^2$-values were obtained by logarithmic interpolation between the above values.

The angular momentum loss rate is

$$\frac{dJ}{dt} = \frac{d(mk^2r^2\Omega)}{dt} = mk^2r^2\frac{d\Omega}{dt} + k^2r^2\Omega\frac{dm}{dt}. \quad (4)$$

On the other hand,

$$\frac{dJ}{dt} = r^2\Omega\frac{dm}{dt}. \quad (5)$$

In these equations, the radius $r$ of the star was assumed to be constant during the W-R phase, and the right-hand side of Equation (5) represents the angular momentum loss from the stellar surface. For helium stars $\gtrsim 8\ M_\odot$ the radii indeed change little during the evolution; for the higher masses the radii shrink somewhat in the course of helium burning, but as this leads to a spin-up of the star, the angular momentum loss rate from the surface will, in first approximation, remain the same. We therefore ignored the radius evolution of the helium stars. Combination of Equations (4) and (5) then leads to

$$\frac{d\ln\Omega}{dt} = \left(\frac{1-k^2}{k^2}\right)\frac{d\ln m}{dt}. \quad (6)$$

Integration yields

$$\frac{\Omega_f}{\Omega_i} = \left(\frac{m_f}{m_i}\right)^{\frac{1-k^2}{k^2}}, \quad (7)$$

where the subscripts $i$ and $f$ indicate the initial and final situations, respectively, and the exponent has a value between 7 and 9. Although these exponents are large, our calculations below show that for low metallicity the value of $m_i/m_f$ remains close to unity over the considerable range of masses.

We applied this equation, in combination with the above-given $f$-values and the wind mass-loss rates and total lifetimes of the helium stars calculated as defined above. We started with helium stars rotating at their breakup values after their formation by a merger and calculated the specific angular momentums $J_\star$ of their collapsing cores at the end of the evolution, for three values of the metallicity, $Z = Z_\odot$, $Z = 0.3\ Z_\odot$, and $Z = 0.1\ Z_\odot$, and for initial helium star masses in the range of 8–100 $M_\odot$. The resulting final specific angular momentums of the collapsing CO cores for these three metallicities are depicted in Figure 2. (The discontinuities in the slope of the curves are in part caused by our interpolation methods combined with the sudden jumps of the $f$-values, $k^2$-values, and values of some other quantities at certain helium star mass values as described above.)

One observes that for solar metallicity the range in zero-age masses that have sufficient final core angular momentum for producing a GRB is considerably smaller than for lower metallicity, but that high metallicities cannot be excluded for SN Ic-BL progenitors. For low metallicity the range in zero-age mass increases, which is consistent with a higher proportion of GRBs at lower metallicity.

The curves show that for solar metallicity, the final specific angular momentums of the cores are sufficient for producing

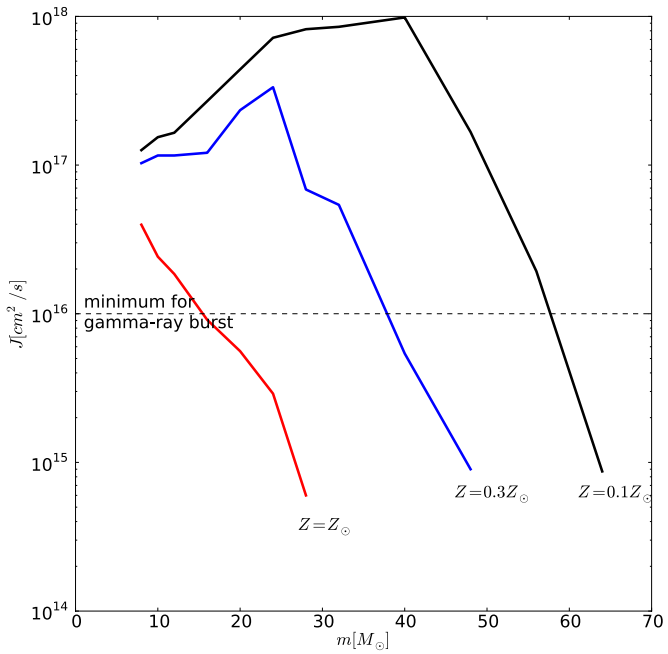


**Figure 2.** Specific core angular momentum $J$ at the end of the evolution of a merger-produced helium star as a function of its zero-age helium main-sequence mass $m$, for solar metallicity, $Z = Z_\odot$ (red), $Z = 0.3Z_\odot$ (blue), and $Z = 0.1Z_\odot$ (black, as indicated). The loss of angular momentum was calculated over the evolution of the W-R phase using the wind parameters by Yoon et al. (2006) with an additional correction for the carbon-W-R phase. At birth, these merger-produced helium stars are assumed to spin at their breakup rotation rate. To produce a gamma-ray burst, a minimum angular momentum of $J = 10^{16}$ cm$^2$ s$^{-1}$ is required (Woosley & Bloom 2006; Kouveliotou et al. 2012; López-Cámara et al. 2010; Woosley & Heger 2012).

(A color version of this figure is available in the online journal.)

LGRBs only in the helium star mass range 8–16 $M_\odot$, for $Z = 0.3\ Z_\odot$ the allowed mass range is 8–38 $M_\odot$, and for $Z = 0.1\ Z_\odot$ the range has widened to 8–61 $M_\odot$.

We thus see that, in principle, SNe Ic-BL and LGRBs can, according to this merger model, be produced at any metallicity, but that the mass range in which such events can be produced is much larger at low metallicity than at high metallicity. We speculate that this is the reason why LGRBs have a preference for occurring at low metallicity but are still occasionally seen in a high-metallicity environment.

We now consider dynamical processes in dense young star clusters that could produce these helium star mergers and collision products that could power the engine of an SN Ic-BL.

## 3. PROPOSED MERGER SCENARIOS FOR DYNAMICALLY PRODUCED BINARIES, RESULTING IN RAPIDLY ROTATING COLLAPSING CO CORES

Our scenario concerns the merger of a dynamically produced binary, consisting of two massive stars that at the time of the merger are in or on their way to core helium burning. To be simultaneously in this phase, the two stars should at the outset not differ much in mass. In the case of low metallicity the stellar-wind mass loss during the hydrogen-burning evolution of the stars will be small, and the two stars will still have hydrogen-rich envelopes when they merge. During hydrogen shell burning, these low-metallicity stars evolve to become red supergiants with very large radii. A binary contains insufficient room for such stars, and a common envelope will ensue in which the two compact cores of the stars spiral toward each other and merge, forming a helium core that rotates near breakup (i.e., with the maximum possible angular momentum). During the common-envelope phase, the hydrogen-rich envelope is ejected, due to the release of a very large amount of gravitational binding energy by the shrinking of the binary orbit (e.g., see Webbink 1984; Ivanova et al. 2013).

In the high-metallicity case, the two massive stars will at the time of the merger already have lost their hydrogen-rich envelopes due to the strong stellar winds and have become W-R stars, but the outcome of the merger will also be a critically rotating helium star. Such an object is also expected to produce an SN Ic-BL. However, to make the two stars merge at this phase requires an extra agent, since such hydrogen-poor stars (W-R stars) have small radii and are not expected to go into a common-envelope phase on their own accord. To make them merge, a third companion to this binary is needed, through the Kozai (1962) effect, in which the exchange of angular momentum between an inclined outer orbit and the tight inner orbit drives the latter to extremely high ($\gtrsim$0.9) eccentricity. This evolution is likely to result in an off-center collision between the two W-R stars, leading to a rapidly rotating helium star.

Both such types of almost-equal-mass systems, without and with a third companion, are expected to be produced by dynamical interactions in dense young star clusters, as numerical studies of star-cluster evolution have shown (Heggie et al. 1996; Portegies Zwart et al. 1999). These studies show that in dense young star clusters the most massive stars rapidly sink to the cluster center, where they tend to form binary systems with components that are very close in mass (Gaburov et al. 2008). Further dynamical interactions with cluster stars and binaries may lead to the expulsion of such a massive binary from the cluster, turning it into a runaway star (Leonard & Duncan 1988; Fujii & Portegies Zwart 2011). The very massive almost-equal-mass binary R145 near the LMC cluster R136 appears to be precisely such a kicked-out runaway binary (Sana et al. 2013) (also the equal-mass close binary Y Cygni, which consists of two equal-mass B0 IV stars, in an eccentric 3 day orbit, is such a runaway star, of lower mass, in our own Galaxy; its cluster of origin is, however, not known; Gies & Bolton 1982). These ejected binaries tend to be the ideal candidates for producing LGRB/SN Ic-BL, and our model therefore predicts that LGRBs/SN Ic-BL can also be found outside, though near (at a distance 300–$10^3$ pc) massive star clusters. This appears indeed to be the case for some of the LGRBs/SN Ic-BL, the prime example being GRB 980425/SN 1998bw (Hammer et al. 2006).

### 3.1. The Link with Dense Young Star Clusters

The above scenario only works for clusters for which a massive star reaches the cluster core and pairs off in a binary before it leaves the main sequence. The most massive star $m_{\rm max}$ in a cluster of mass $M$ is $m_{\rm max} \simeq 1.2(M/M_\odot)^{0.45}\ M_\odot$ (Weidner & Kroupa 2004) with a maximum of about 150 $M_\odot$ (Massey & Hunter 1998; Figer 2005). In our case, however, the helium core of the most massive star, before merger, should be $\lesssim$30 $M_\odot$ (Figure 2), such that the two cores together form a helium star $\lesssim$60 $M_\odot$. This implies that the zero-age main-sequence (ZAMS) hydrogen-rich progenitors should have been less massive than about 61–68 $M_\odot$. (The range here reflects the uncertainty in the moment when the common-envelope ensues, which translates into a range of core masses at the onset of Roche lobe overflow.) This corresponds to a cluster mass of 6200–7900 $M_\odot$. In order to be able to form a binary, the star has to sink from the cluster

virial radius $R$ to the cluster center within its main-sequence lifetime. This happens on a dynamical friction timescale (Binney & Tremaine 1987; here we adopted for the Coulomb logarithm $\log(\Lambda) = \log(0.1N)$):

$$t_{\rm df} \simeq 2.2\,{\rm Myr}\left(\frac{R}{\rm pc}\right)^{3/2}\left(\frac{M}{10^4\,M_\odot}\right)^{1./2}\left(\frac{m_{\rm max}}{150\,M_\odot}\right)^{-1}. \quad (8)$$

By this time the most massive stars have sunken to the cluster center. A single massive star, or one in a binary system, will upon arrival in the central portion of the star cluster acquire a companion of similar mass to form a binary or higher-order system (Heggie et al. 1996; Gaburov et al. 2008). A newly formed binary will at first be rather wide, with a binding energy comparable to the mean kinetic energy of the stars, or ∼1 kT. Repeated interactions with other cluster members drive the hardening of the binary to $\gtrsim$100 kT. In a number of cases, such a binary in the cluster center may dynamically acquire a third companion, which later in life, through the Kozai (1962) effect, may lead to a collision of the inner pair.

In Figure 3 we present a number of observed star clusters from the compilation of Portegies Zwart et al. (2010). The red dashed curve indicates the cluster parameters, mass $M$ and (virial/effective) radius $R$, for which the dynamical friction timescale Equation (8) equals the main-sequence lifetime of the most massive star. Clusters that are born with parameters below this curve are prone to quick mass segregation and form the relevant population for SNe producing type SN Ic-BL progenitor binaries.

The young and dense galactic star cluster NGC 3603 is in the regime for this process and may produce an SN Ic-BL. The cluster contains a 3.77 day double-lined eclipsing binary with a $116 \pm 31\ M_\odot$ primary star NGC 3603-A1 and a secondary star of $89 \pm 16\ M_\odot$ (Schnurr et al. 2008), which could be a prototypical example of such a binary, although, just like in the Quintuple cluster (Figer et al. 1999), its metallicity may be too high to produce an LGRB (see Figure 2). Several of the most massive stars in the Quintuplet cluster are known to be binaries, but orbital parameters have not yet been determined (Liermann et al. 2012). The central star cluster R136 in the 30 Doradus region of the LMC may be sufficiently dense to produce an SN Ic-BL, although the observed parameters are controversial; in Figure 3 we adopted those reported by Selman & Melnick (2013). This cluster may have ejected the object R144, which Fujii & Portegies Zwart (2011) predicted to be a massive binary. Recently, Sana et al. (2013) identified R144 as a $\lesssim$370 day spectroscopic binary with a total mass of ∼200–300 $M_\odot$, confirming this earlier prediction.

The densest star clusters experience core collapse shortly after birth. This happens in a small fraction of the two-body relaxation time $t_{\rm cc} \sim 0.15 t_{\rm rlx}$ (Portegies Zwart & McMillan 2002; Gürkan et al. 2006), as long as this timescale does not exceed the main-sequence lifetime of the most massive star; otherwise, the cluster will expand due to copious stellar mass loss. Here the relaxation time of a cluster with effective (virial) radius $R$ and mean stellar mass $\langle m\rangle \equiv M/N$ is

$$t_{\rm cc} \simeq 3.0\,{\rm Myr}\left(\frac{M}{10^4\,M_\odot}\right)^{1/2}\left(\frac{R}{\rm pc}\right)^{3/2}\left(\frac{\langle m\rangle}{M_\odot}\right)^{-1}. \quad (9)$$

The red solid curve in Figure 3 indicates the cluster parameters, mass $M$ and (virial) radius $R$, for which the core-collapse timescale (Equation (9)) equals the main-sequence lifetime of the most massive star.

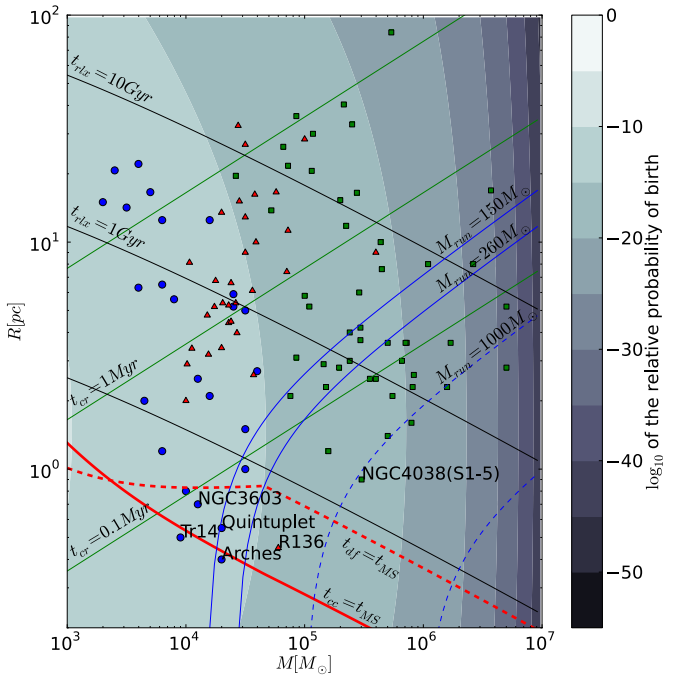


**Figure 3.** Mass and effective radius for young clusters. The gray-shaded black and green curves are reproduced from Figure 1. The blue bullets, red triangles, and green squares indicate the population of observed helium star clusters in the Milky Way, in the Local Group, and from nearby galaxies, respectively. The data were taken from Tables 1 (blue), 2 (red), and 3 (green) of Portegies Zwart et al. (2010), except for the parameters for R136 (which are from Selman & Melnick 2013), Tr14 (from Hußmann et al. 2012), and the Antennae cluster S1_5 (Mengel et al. 2008). Several of the densest clusters are identified by their common name. The red dashed curve gives the radius of clusters for which the dynamical friction timescale of the most massive star is the same as its main-sequence lifetime. SNe Ic-BL are expected to occur in clusters in the region below the dashed red curve, as long as they have a relatively low mass of $\lesssim$7900 $M_\odot$. The solid red curve indicates the radius of clusters for which the core-collapse timescale is the same as the main-sequence lifetime of the most massive star. The blue curves (from bottom to the right side) indicate the mass of a collision runaway that can form in these clusters. Two of these curves are identified as $M_{\rm run} = 150\,M_\odot$ and $M_{\rm run} = 260\,M_\odot$. (The two dashed blue curves indicate $M_{\rm run} = 1000\,M_\odot$ and $M_{\rm run} = 10^4\,M_\odot$.) To the right of the 260 $M_\odot$ massive runaway curve and below the solid red curve, we expect star clusters to produce massive runaways that explode as SLSN-I or SLSN-II. Clusters in the region between the two blue curves and below the solid red curve are expected to produce an SLSN-R.

(A color version of this figure is available in the online journal.)

Clusters that experience core collapse before their most massive stars have left the main sequence are prone to many strong dynamical interactions in the cluster center and may experience a collision runaway. The collision rate during the time between core collapse and the SN explosion of the collision runaway product determines the maximum mass of the latter. Portegies Zwart & McMillan (2002) estimated the mass of a collision runaway as

$$M_{\rm run} = 0.01M\left(1 + \frac{t_{\rm rlx}}{100\,{\rm Myr}}\right)^{-1}, \quad (10)$$

with the additional requirement that $t_{\rm cc} < t_{\rm MS}(m_{\rm max})$. The upper (leftmost) blue curve in Figure 3 indicates the cluster parameters for which a collision runaway leads to a single object with a mass in excess of that of the most massive main-sequence star ($M_{\rm run} \gtrsim 150\,M_\odot$). Clusters to the left of this curve but below the solid red curve will not grow a massive runaway, but repeated interactions in the core may lead to the ejection of the most massive binary, as a high-velocity runaway. Although ejected,

**Table 1**
Event Rates for Families of Supernovae

| SN Type | Metallicity | Observed | Model CBG ($\beta = -2$, $\langle r \rangle = 3$pc) | Model MWG ($\beta = -3$, $\langle r \rangle = 5$pc) | Combined 1:10 Ratio |
|---|---|---|---|---|---|
| LGRB/SN Ic-BL | $Z = 0.1\,Z_\odot$ | $0.8 \times 10^{-3}$ | $(7.1 \pm 0.1) \times 10^{-3}$ | $2.9 \times 10^{-3}$ | $3.3 \times 10^{-3}$ |
| LGRB/SN Ic-BL | $Z = 0.3\,Z_\odot$ | $1.0 \times 10^{-3}$ | $(6.5 \pm 0.2) \times 10^{-3}$ | $2.8 \times 10^{-3}$ | $3.1 \times 10^{-3}$ |
| LGRB/SN Ic-BL | $Z = Z_\odot$ | $0.2 \times 10^{-3}$ | $(3.0 \pm 0.6) \times 10^{-3}$ | $1.5 \times 10^{-3}$ | $1.6 \times 10^{-3}$ |
| SLSN-I/II | $\forall Z$ | $1.7 \times 10^{-4}$ | $3.4 \times 10^{-5}$ | $2.3 \times 10^{-7}$ | $3.4 \times 10^{-6}$ |
| SLSN-R | $\forall Z$ | $2 \times 10^{-5}$ | $4.6 \times 10^{-5}$ | $7.0 \times 10^{-7}$ | $4.6 \times 10^{-6}$ |

**Notes.** Observed rates (third column) for SLSNe are from Gal-Yam (2012), and we determined the relative rate for LGRB/SN Ic-BL from the statistics by Levesque et al. (2010a), from a sample of 14 LGRBs with a range of metallicities. The subsequent three columns give the various rates from our model calculations. All the rates are normalized to the core collapse supernova (type II) rate. The best values are from our adopted Schechter mass function with exponential mass dependency of $\beta \gtrsim -2$ and with a lognormal size distribution with mean of $\langle r \rangle = 3$ pc, which represents the star clusters in blue compact dwarf galaxies. The Milky Way fits best with $\beta \lesssim -3$ and $\langle r \rangle = 5$ pc. The characteristic mass in the Schechter function in both cases is $M_* = 2 \times 10^5\ M_\odot$. The last column gives a combined rate assuming a relative ratio in starburst-to-quiescent galaxies of 1:10 (Lamastra et al. 2013).

these binaries are still consistent with the earlier discussed SN Ic-BL/LGRB progenitors. We therefore speculate that clusters born in this range of parameters are likely to produce SN Ic-BL that, by the time of the exploding star, are outside the cluster. With a typical velocity of $\gtrsim$100 km s$^{-1}$ and within $\sim$3 Myr to travel, the SN type SN Ic-BL may occur $\gtrsim$300 pc from the cluster.

The young and dense Galactic star cluster Trumpler 14 is in the proper regime of parameter space for producing an SN Ic-BL by a dynamically formed massive binary in its center. Although the cluster is still too young to have experienced core collapse, a massive binary is already present (Mason et al. 2009). Based on our analysis, we expect that the binary in Trumpler 14 will eventually be ejected from the cluster center and produce an SN at some distance away, but due to the high metallicity of Tr 14, this explosion will probably not resemble an LGRB/SN Ic-BL.

According to our model each of these clusters is a candidate for producing an SN Ic-BL, each of which is expected to go off within the next 3 Myr, totaling a rate of $\sim$1 Myr$^{-1}$, or $\sim 10^{-4}$ of the type II SN rate. In Table 1 we calculate the rate for SN type SN Ic-BL from the galactic star cluster population and arrive at a theoretical upper limit of $1.5 \times 10^{-3}$ yr$^{-1}$.

## 4. THE ORIGIN OF SLSNe

Dense clusters that are more massive than indicated by the leftmost blue curve in Figure 3 but below the solid red curve are prone to producing an unusually massive star via a collision runaway (Portegies Zwart & McMillan 2002). In relatively compact ($R \lesssim 0.4$ pc) and low-mass ($M \lesssim 20{,}000$–$30{,}000\ M_\odot$) star clusters the collision runaway product can reach a mass of 150–260 $M_\odot$ (Portegies Zwart & van den Heuvel 2007). (According to Yungelson et al. 2008, these limits are somewhat higher and occur between 250 and 800 $M_\odot$.) These stars collapse in a luminous pair-instability SN (Rakavy & Shaviv 1967; Langer et al. 2007; Scannapieco 2009; Cooke et al. 2012), giving rise to a SLSN-R, because these SNe produce large amounts of $^{56}$Ni, as was proposed for SN 2007bi by Pan et al. (2012). The Arches star cluster is located in the regime of forming a $\sim$170 $M_\odot$ collision runaway star, which is in the range for leading to a pair instability SN.

Overplotted in Figure 3 (gray shades) is the probability density function at which star clusters are born in the Galaxy. The gray shading is identical to that in Figure 1, but reproduced here to complement the impression of cluster birth parameters (in gray) with the observed population of star clusters. For the size distribution of the clusters, we fitted the observed distribution of cluster sizes (taken from Tables 2– 4 of Portegies Zwart et al. 2010) to a lognormal distribution, which gave a satisfactory fit for a mean radius of 5 pc and a dispersion of 3 pc. For the initial mass function of young clusters, we adopted a Schechter function (Schechter 1976) with a minimum mass of $M = 500\ M_\odot$ and a characteristic mass of $2 \times 10^5\ M_\odot$ (Larsen 2009). The exponential falloff in the Schechter mass function for spiral galaxies is $\beta \lesssim -3$ (see Equation (1)), whereas for dwarf starburst galaxies it is $\beta \gtrsim -2$. This difference in shape of the mass function, together with the adopted variation in the size distribution, gives rise to a dramatic difference in the densities for these clusters (see Table 1).

In sufficiently dense star clusters of $>30{,}000\ M_\odot$ the collision runaway can grow to a mass $>260\ M_\odot$ (in Figure 3 the area to the right of the rightmost solid blue curve and below the sold red curve). We speculate that these extremely massive stars produce SLSN-I/II by collapsing to a black hole of intermediate mass (Scannapieco 2009). The mass of the collision runaway can reach values of up to a few $\times 10^3\ M_\odot$ (Portegies Zwart & McMillan 2002). By the time the star experiences an SN, it has shed most of its mass again in a dense stellar wind (Belkus et al. 2007; Yungelson et al. 2008; Glebbeek et al. 2009) and it is uncertain how much mass eventually collapses to the black hole (Belkus et al. 2007). Integrating over the mass and size distributions for star clusters, we derive a rate of $\mathcal{R}_{\rm SLSN\text{-}I/II} \simeq 2.3 \times 10^{-7}$ for the Milky Way population. By adopting the same size distribution and mass distribution of star clusters as we did before for the population of clusters in blue compact dwarf galaxies, we arrive at a rate of $\mathcal{R}_{\rm SLSN\text{-}I/II} \simeq 3.4 \times 10^{-5}$, which is somewhat smaller than the observed rate for combined types SLSN-I and SLSN-II.

## 5. DISCUSSION

We can calculate event rates for SNe Ic-BL, SLSN-R, and SLSN-I/II by integrating the probability density function of star cluster birth parameters and over galaxy types. The integrated rates for a large spiral galaxy and dwarf starburst galaxies are presented in Table 1. The SN Ic-BL are calculated

by integrating the area below the dashed red curve in Figure 3. Because it is in our model the most massive star in a cluster that pairs off and produces an SN Ic-BL, we adopt an upper limit for the most massive star in the cluster and integrate up to that cluster mass.

According to our analysis presented in Figure 2, the appropriate helium core mass for each of the merging stars should be at most ~8, 16, and 30 $M_\odot$ for $Z = Z_\odot$, $Z = 0.3\,Z_\odot$, and $Z = 0.1\,Z_\odot$, respectively. Such core masses are reached in ZAMS stars of at least 23–26 $M_\odot$, 42–48 $M_\odot$, and 61–68 $M_\odot$. This mass relates to the most massive star born in clusters, which then should not exceed 700–900 $M_\odot$, 2700–3600 $M_\odot$, and 6200–7900 $M_\odot$ for $Z = Z_\odot$, $Z = 0.3\,Z_\odot$, and $Z = 0.1\,Z_\odot$, respectively. The lower metallicities correspond to the higher mass limits for the ZAMS stars and consequently also for the upper limit in the cluster mass range; SN Ic-BL are expected to occur in relatively low-mass ($\lesssim$7900 $M_\odot$) star clusters. (Note, however, that these maximum cluster masses are based on the assumption that the helium star merger product lives the complete helium main-sequence lifetime for its mass. Merger products of binaries with mass ratios 0.85 to 0.90 live only about half this lifetime, and thus undergo much less angular momentum loss by wind, leading for each metallicity to considerably higher upper mass limits for becoming LGRBs, and thus also to higher allowed cluster masses.)

In Table 1 we compare the relative rates for LGRB/SN Ic-BL as a function of metallicity with the metallicity dependency in the observed rates, using statistics of LGRBs by Levesque et al. (2010a; see also Wolf & Podsiadlowski 2007). Although these statistics contain only 14 LGRBs, the number of low (with an oxygen abundance of $12 + \log(\mathrm{O/H}) < 8.2$ counting five LGRBs), medium (7), and high ($12 + \log(\mathrm{O/H}) > 8.7$ with two LGRBs) metallicity poses an interesting relation that can be compared with our model calculations. The total relative rate for LGRB/SN Ic BL was fixed at $2 \times 10^{-3}$ (Fruchter et al. 2006).

The event rate for SN type SLSN-I/II is calculated by integrating the area below the solid red curve and to the right of the rightmost solid blue curve, and the type SLSN-R rate is obtained by integrating between the two solid blue curves and below the solid red curve. We normalized to the SN type II rate by counting the number of stars between 8 and 25 $M_\odot$, and we adopted a minimum cluster mass of 150 $M_\odot$. The relative rates for the various types of SNe are presented in Table 1.

The rate of the various events for a galaxy similar to the Milky Way is more than one order of magnitude lower than the observed rate or the rate derived for compact dwarf galaxies. The relative proportion of star formation in these various types of galaxies may easily be an order of magnitude, major spiral galaxies dominating this rate (Lamastra et al. 2013). In that case, the rate for SN type Ic-BL may still be dominated by large spiral galaxies compared to compact dwarf galaxies, but for the superluminal SNe this does not pose a discrepancy.

The difference in the observed rates of types SLSN-I/II compared to SLSN-R is about an order of magnitude, whereas in our models they are comparable. The relative ratio between SLSN-I/II and SLSN-R can easily be tuned by moving the boundaries in runaway mass between producing an SLSN-R and an SLSN-I/II. Adopting a lower limit to the mass of the collision runaway to produce an SLSN-I/II of ~180 $M_\odot$ (instead of 260 $M_\odot$) would solve this discrepancy.

We do not explicitly make the distinction between type SLSN I and type II, but derive the total rate. Upon each collision several $M_\odot$ of hydrogen is injected into the collision runaway, but this mass is blown away in the copious stellar wind in a few $\times 10^4$ yr. A collision between the runaway and a hydrogen-rich star shortly before the SN of the former was proposed by Portegies Zwart & van den Heuvel (2007) to explain the SLSN-II 2006gy, which occurred close to the nucleus of a large galaxy (Quimby 2006). The ratio between the timescale on which fresh hydrogen is injected into the collision runaway and the time required to deplete the newly acquired hydrogen envelope determines the ratio of SLSNe type II relative to SLSNe type I. The observed comparable rates of type SLSN-II relative to SLSN-I are consistent with this regime of collisional growth (Portegies Zwart & McMillan 2002). Both the rates for SLSN-R and for SLSN-I/II increase if a higher proportion of star clusters are born with high density, as is the case for clusters in blue compact dwarf galaxies compared to the Milky Way.

The intermediate-mass black hole that forms through an SLSN-I/II is expected to be located in the dense core of a collapsed star cluster. In the core of such a star cluster the intermediate-mass black hole is likely to be accompanied by another star, or otherwise it is likely to acquire one within a core relaxation timescale. The orbital period of such a binary typically is in the range of 50–500 days (Patruno et al. 2006). The observational repercussions of a massive black hole that is orbited by another massive star are profound and could be characterized by a peculiar X-ray emission. The companion eventually will leave the main sequence upon which Roche lobe overflow is likely to ensue. Such a phase of mass transfers from the captured star to the intermediate-mass black hole may lead to an ultraluminous X-ray source, much like the observed systems M82 X-1 (Kaaret et al. 2001), NGC 1313 X-2 (Zampieri & Patruno 2011), HLX-1 (Webb et al. 2012), NGC 5408 X-1 (Strohmayer 2009), and NGC 7479 X-1 (Voss et al. 2011). The observed periodicity in M82 X-1 (62 days), NGC 5408 X-1 (115 days), and HLX-1 (388 days) and their X-ray fluxes are consistent with a cluster member being captured by an intermediate-mass black hole and feeding the latter via a dense stellar wind or Roche lobe overflow.

It is a pleasure to thank the anonymous referee for the constructive remarks for improving the manuscript and Daniel Schearer and Nathan de Vries for discussions. This work was supported by the Netherlands Research Council NWO (grants #643.200.503 [LGM], #639.073.803 [VICI], and #614.061.608 [AMUSE]), by the National Science Foundation under Grant No. NSF PHY11-25915, and by the Netherlands Research School for Astronomy (NOVA).

## REFERENCES

Arnett, W. D. 1978, ApJ, 219, 1008
Bate, M. R. 2009, MNRAS, 397, 232
Belkus, H., Van Bever, J., & Vanbeveren, D. 2007, ApJ, 659, 1576
Binney, J., & Tremaine, S. 1987, Galactic Dynamics (Princeton, NJ: Princeton Univ. Press), 747
Bogomazov, A. I., Lipunov, V. M., & Tutukov, A. V. 2007, ARep, 51, 308
Brunt, C. M., Heyer, M. H., & Mac Low, M.-M. 2009, A&A, 504, 883
Cano, Z., Bersier, D., Guidorzi, C., et al. 2011, ApJ, 740, 41
Conti, P. S., Crowther, P. A., & Leitherer, C. 2008, From Luminous Hot Stars to Starburst Galaxies (Cambridge: Cambridge Univ. Press)
Cooke, J., Sullivan, M., Gal-Yam, A., et al. 2012, Natur, 491, 228
Deinzer, W., & Salpeter, E. E. 1964, ApJ, 140, 499
Detmers, R. G., Langer, N., Podsiadlowski, P., & Izzard, R. G. 2008, A&A, 484, 831
Drake, A. J., Djorgovski, S. G., Mahabal, A., et al. 2011, ApJ, 735, 106
Federrath, C., & Klessen, R. S. 2012, ApJ, 761, 156
Figer, D. F. 2005, Natur, 434, 192
Figer, D. F., McLean, I. S., & Morris, M. 1999, ApJ, 514, 202
Fruchter, A. S., Levan, A. J., Strolger, L., et al. 2006, Natur, 441, 463

Fryer, C. L., Mazzali, P. A., Prochaska, J., et al. 2007, PASP, 119, 1211
Fujii, M. S., & Portegies Zwart, S. 2011, Sci, 334, 1380
Gaburov, E., Gualandris, A., & Portegies Zwart, S. 2008, MNRAS, 384, 376
Galama, T. J., Vreeswijk, P. M., van Paradijs, J., et al. 1998, Natur, 395, 670
Gal-Yam, A. 2012, Sci, 337, 927
Gehrels, N., & Mészáros, P. 2012, Sci, 337, 932
Gies, D. R., & Bolton, C. T. 1982, ApJ, 260, 240
Glebbeek, E., Gaburov, E., de Mink, S. E., Pols, O. R., & Portegies Zwart, S. F. 2009, A&A, 497, 255
Graham, J. F., & Fruchter, A. S. 2013, ApJ, 774, 119
Gürkan, M. A., Fregeau, J. M., & Rasio, F. A. 2006, ApJL, 640, L39
Hadfield, L. J., & Crowther, P. A. 2006, MNRAS, 368, 1822
Hammer, F., Flores, H., Schaerer, D., et al. 2006, A&A, 454, 103
Hao, J.-M., & Yuan, Y.-F. 2013, ApJ, 772, 42
Heggie, D. C., Hut, P., & McMillan, S. L. W. 1996, ApJ, 467, 359
Hußmann, B., Stolte, A., Brandner, W., Gennaro, M., & Liermann, A. 2012, A&A, 540, A57
Ivanova, N., Justham, S., Chen, X., et al. 2013, A&ARv, 21, 59
Iwamoto, K., Mazzali, P. A., Nomoto, K., et al. 1998, Natur, 395, 672
Kaaret, P., Prestwich, A. H., Zezas, A., et al. 2001, MNRAS, 321, L29
Kaaret, P., Schmitt, J., & Gorski, M. 2011, ApJ, 741, 10
Kasen, D., & Bildsten, L. 2010, ApJ, 717, 245
Kelly, P. L., & Kirshner, R. P. 2012, ApJ, 759, 107
Kouveliotou, C., Wijers, R. A. M. J., & Woosley, S. 2012, Gamma-ray Bursts (Cambridge: Cambridge Univ. Press)
Kozai, Y. 1962, AJ, 67, 591
Lamastra, A., Menci, N., Fiore, F., & Santini, P. 2013, A&A, 552, A44
Langer, N., & Norman, C. A. 2006, ApJL, 638, L63
Langer, N., Norman, C. A., de Koter, A., et al. 2007, A&A, 475, L19
Larsen, S. S. 2009, A&A, 503, 467
Leonard, P. J. T., & Duncan, M. J. 1988, AJ, 96, 222
Levesque, E. M., Kewley, L. J., Berger, E., & Zahid, H. J. 2010a, AJ, 140, 1557
Levesque, E. M., Soderberg, A. M., Kewley, L. J., & Berger, E. 2010b, ApJ, 725, 1337
Liermann, A., Hamann, W.-R., & Oskinova, L. M. 2012, A&A, 540, A14
Lim, S., Hwang, N., & Lee, M. G. 2013, ApJ, 766, 20
López-Cámara, D., Lee, W. H., & Ramirez-Ruiz, E. 2010, ApJ, 716, 1308
MacFadyen, A. I., & Woosley, S. E. 1999, ApJ, 524, 262
Mason, B. D., Hartkopf, W. I., Gies, D. R., Henry, T. J., & Helsel, J. W. 2009, AJ, 137, 3358
Massey, P., & Hunter, D. A. 1998, ApJ, 493, 180
McKee, C. F., & Ostriker, E. C. 2007, ARA&A, 45, 565
Mengel, S., Lehnert, M. D., Thatte, N. A., et al. 2008, A&A, 489, 1091
Metzger, B. D., Giannios, D., Thompson, T. A., Bucciantini, N., & Quataert, E. 2011, MNRAS, 413, 2031
Moeckel, N., & Bate, M. R. 2010, MNRAS, 404, 721
Padoan, P., Juvela, M., Kritsuk, A., & Norman, M. L. 2009, ApJL, 707, L153
Pan, T., Loeb, A., & Kasen, D. 2012, MNRAS, 423, 2203
Patruno, A., Portegies Zwart, S., Dewi, J., & Hopman, C. 2006, MNRAS, 370, L6
Paxton, B., Bildsten, L., Dotter, A., et al. 2011, ApJS, 192, 3
Portegies Zwart, S., McMillan, S. L. W., van Elteren, E., Pelupessy, I., & de Vries, N. 2013, CoPhC, 183, 456
Portegies Zwart, S. F., Makino, J., McMillan, S. L. W., & Hut, P. 1999, A&A, 348, 117
Portegies Zwart, S. F., & McMillan, S. L. W. 2002, ApJ, 576, 899
Portegies Zwart, S. F., McMillan, S. L. W., & Gieles, M. 2010, ARA&A, 48, 431
Portegies Zwart, S. F., & van den Heuvel, E. P. J. 2007, Natur, 450, 388
Quimby, R. 2006, CBET, 644, 1
Rakavy, G., & Shaviv, G. 1967, ApJ, 148, 803
Sana, H., van Boeckel, T., Tramper, F., et al. 2013, MNRAS, 432, L26
Savonije, G. J., & van den Heuvel, E. P. J. 1977, ApJL, 214, L19
Scannapieco, E. 2009, Pair-production Supernovae: Theory and Observation (Cambridge: Cambridge Univ. Press), 209
Schechter, P. 1976, ApJ, 203, 297
Schnurr, O., Casoli, J., Chené, A.-N., Moffat, A. F. J., & St-Louis, N. 2008, MNRAS, 389, L38
Selman, F. J., & Melnick, J. 2013, A&A, 552, A94
Soderberg, A. M., Chakraborti, S., Pignata, G., et al. 2010, Natur, 463, 513
Spruit, H. C. 2002, A&A, 381, 923
Strohmayer, T. E. 2009, ApJL, 706, L210
van den Heuvel, E. P. J., & Yoon, S.-C. 2007, Ap&SS, 311, 177
Voss, R., Nielsen, M. T. B., Nelemans, G., Fraser, M., & Smartt, S. J. 2011, MNRAS, 418, L124
Webb, N., Cseh, D., Lenc, E., et al. 2012, Sci, 337, 554
Webbink, R. F. 1984, ApJ, 277, 355
Weidner, C., & Kroupa, P. 2004, MNRAS, 348, 187
Wolf, C., & Podsiadlowski, P. 2007, MNRAS, 375, 1049
Woosley, S. E. 1993, ApJ, 405, 273
Woosley, S. E. 2010, ApJL, 719, L204
Woosley, S. E., & Bloom, J. S. 2006, ARA&A, 44, 507
Woosley, S. E., & Heger, A. 2012, ApJ, 752, 32
Yoon, S.-C., & Langer, N. 2005, A&A, 443, 643
Yoon, S.-C., Langer, N., & Norman, C. 2006, A&A, 460, 199
Yungelson, L. R., van den Heuvel, E. P. J., Vink, J. S., Portegies Zwart, S. F., & de Koter, A. 2008, A&A, 477, 223
Zampieri, L., & Patruno, A. 2011, AN, 332, 422
Zhang, B., & Yan, H. 2011, ApJ, 726, 90